

## Apigenin ameliorates HFD-induced NAFLD through regulation of the XO/NLRP3 pathways☆

Yanan Lv<sup>a</sup>, Xiaona Gao<sup>a</sup>, Yan Luo<sup>b</sup>, Wentao Fan<sup>a</sup>, Tongtong Shen<sup>a</sup>, Chenchen Ding<sup>a</sup>, Ming Yao<sup>a</sup>, Suquan Song<sup>a,\*</sup>, Liping Yan<sup>a,c,\*</sup>

<sup>a</sup>MOE Joint International Research Laboratory of Animal Health and Food Safety, College of Veterinary Medicine, Nanjing Agricultural University, Nanjing, 210095, Jiangsu Province, China

<sup>b</sup>Administration for Market Regulation of Guangdong Province Key Laboratory of Supervision for Edible Agricultural Products, Shenzhen Centre of Inspection and Testing for Agricultural Products, Shenzhen 518000, Guangdong Province, China

<sup>c</sup>Jiangsu Engineering Laboratory of Animal Immunology, Institute of Immunology and College of Veterinary Medicine, Nanjing Agricultural University, Nanjing, 210095, Jiangsu Province, China

Received 28 December 2018; received in revised form 21 May 2019; accepted 21 May 2019

### Abstract

Non-alcoholic fatty liver disease (NAFLD) is the most common cause of liver-related morbidity and mortality disease in the world. However, no effective pharmacological treatment for NAFLD has been found. In this study, we used a high fat diet (HFD)-induced NAFLD model to investigate hepatoprotective effect of apigenin (API) against NAFLD and further explored its potential mechanism. Our results demonstrated that gavage administration of API could mitigate HFD-induced liver injury, enhance insulin sensitivity and markedly reduce lipid accumulation in HFD-fed mice livers. In addition, histological analysis showed that hepatic steatosis and macrophages recruitment in the API treatment group were recovered compared with mice fed with HFD alone. Importantly, API could reverse the HFD-induced activation of the NLRP3 inflammasome, further reduced inflammatory cytokines IL-1 $\beta$  and IL-18 release, accompanied with the inhibition of xanthine oxidase (XO) activity and the reduction of uric acid and reactive oxygen species (ROS) production. The pharmacological role of API was further confirmed using free fatty acid (FFA) induced cell NAFLD model. Taking together, our results demonstrated that API could protect against HFD-induced NAFLD by ameliorating hepatic lipid accumulation and inflammation. These protective effects may be partially attributed to the regulation of XO by API, which further modulated NLRP3 inflammasome activation and inflammatory cytokines IL-1 $\beta$  and IL-18 release. Therefore API is a potential therapeutic agent for the prevention of NAFLD.

© 2019 Elsevier Inc. All rights reserved.

**Keywords:** NAFLD; Xanthine oxidase; NLRP3 inflammasome; Apigenin; High-fat diet; Free fatty acid

### 1. Introduction

Non-alcoholic fatty liver disease (NAFLD) is the most common cause of liver-related morbidity and mortality [1,2], which encompasses an abroad disease spectrum, including simple steatosis, nonalcoholic steatohepatitis (NASH), fibrosis, irreversible cirrhosis, and even hepatocellular carcinoma [3]. It is worth noting that, besides liver, NAFLD could also contribute to the onset of disease in other organs [4],

such as type 2 diabetes mellitus (T2DM) [5], cardiovascular (CVD) and cardiac diseases [6], and chronic kidney disease (CKD) [7]. Because the pathogenesis of NAFLD remains unclear, few long-term efficacies and safety approaches are available for NAFLD treatment so far [8].

Xanthine oxidase (XO), plays a key role in purine nucleotide degradation, which catalyze the production of uric acid and reaction oxygen species (ROS) from hypoxanthine [9]. As we known, XO is a well-established therapeutic target for hyperuricemia, and it is also involved in lipogenesis and atherosclerosis [10,11]. XO is highly expressed in liver, indicating the potential organ-specific physiological function of the enzyme [12]. Emerging studies indicated that XO played a significant role in the pathogenesis of NAFLD. Either knocking down or inhibiting XO could significantly inhibit uric acid production, and attenuate hepatocyte fat accumulation in a FFA-induced cellular model of NAFLD, while overexpression of XO showed the opposite results [13]. Therefore targeting XO may represent a therapeutic approach for treating steatohepatitis. In addition, uric acid-dependent regulation of mitochondrial function was critical for the modulation of lipid homeostasis in fatty liver disease [14] and elevating uric acid in serum level could significantly increase the risk of NAFLD [15]. As the other

\* Funding source: This work was supported by the National Key R&D Program (2016YFD0501009 and 2016YFD0501200), the Natural Science Foundation of Jiangsu Province (BK20161452), the Fundamental Research Funds for the Central Universities (KYZ201848), the Priority Academic Program Development of Jiangsu Higher Education Institutions, the NAU International Cooperation and Cultivation Project (2018-AF-20) and the Key Program of Science and Technology Planning of Guangdong Province (2017B020202010).

\* Corresponding author. Tel.: +86 25 84395789; fax: +86 25 84395166.

E-mail addresses: [suquan.song@njau.edu.cn](mailto:suquan.song@njau.edu.cn) (S. Song), [yanliping@njau.edu.cn](mailto:yanliping@njau.edu.cn) (L. Yan).

main product of XO catalytic reaction, ROS can mediate the peroxidation of lipid, and trigger the occurrence of and progression of NAFLD [16]. Therefore, exploring a safer XO inhibitor may represent a therapeutic approach for the treatment of NAFLD.

Many studies showed that the NOD-like receptor family pyrin domain containing 3 (NLRP3) inflammasome was important in the pathogenesis of NAFLD [17–21]. NLRP3 inflammasome, a multiprotein scaffold, can sense a wide range of danger signals, activate caspase-1 and lead to the processing and secretion of the pro-inflammatory cytokines interleukin-1 $\beta$  (IL-1 $\beta$ ) and IL-18 at last [22–24]. It is reported that XO blockade could impair IL-1 $\beta$ /caspase-1 secretion [25], indicating that NLRP3 inflammasome activation may be essential for the regulatory effect of XO [13]. Furthermore, both uric acid and ROS can stimulate the formation of the NLRP3 inflammasome and mediate secretion of IL-1 $\beta$  and IL-18, which then induce hepatic steatosis and insulin resistance [24–27]. Based on this study, we speculated that the regulation of NLRP3 inflammasome was important for liver damage, and XO was a key regulator of NLRP3 inflammasome in NAFLD.

Apigenin (API) is a naturally occurring bioflavonoid, which is commonly present in fruits, vegetables, herbs and spices [28]. API has diverse pharmacological activities such as anti-oxidation ability [29], anti-inflammatory activity [30], antitumor activities [31] and antidepressant-like efficacy [32]. Many studies have demonstrated that API has effects on anti-obesity and anti-diabetic [33,34]. In addition, API could improve glucose homeostasis, glucose tolerance and hepatic lipid metabolism in mice fed a high-fat diet (HFD) [35]. However, the underlying molecular mechanism of API's hepatoprotective effects against NAFLD remains unclear. In this study, we investigated the role of XO in HFD-induced NAFLD and clarified the mechanisms of API to treat NAFLD. Our findings would provide new insights into the mechanisms underlying the pharmacological effects of API on NAFLD, which would no doubt contribute to novel strategies for the management of diet-induced NAFLD.

## 2. Materials and methods

### 2.1. Chemicals, reagents, and antibodies

API was purchased from Solarbio (Beijing, China). Allopurinol (ALL) was from Sigma (MO, USA). TRIZOL reagent and AceQ qPCR SYBR Green Master Mix were from Vazyme (Nanjing, China). Lysis buffer (RIPA; PMSF, 1:9) was from Beyotime (Shanghai, China). RNA reverse transcription kit and PCR Mix were obtained from Thermo (Waltham, USA). The kits for analysis of ROS, malondialdehyde (MDA), total cholesterol (TC), triglyceride (TG), aspartate aminotransferase (AST), alanine aminotransferase (ALT), and Oil Red O Stain kit were purchased from Jiancheng Bioengineering Institute (Nanjing, China). MTT was from Solarbio (Beijing, China). **ELISA kits for IL-18 and IL-1 $\beta$  and were provided by Enzyme-linked Biotechnology Co., Ltd. (Shanghai, China).** Rabbit-derived polyclonal antibody against NLRP3 and Pro-caspase-1 were from Abcam (Cambridge, UK). Rabbit anti-ASC polyclonal antibody and rabbit anti-caspase-1 P10 polyclonal antibody were provided by OmnimAbs (California, USA).  $\beta$ -Actin antibodies were from Absin (Shanghai, China). Goat anti-rabbit HRP-linked antibodies were purchased from CST (MA, USA). All reagents used in the study were of analytical grade.

### 2.2. Mice and treatment

Male C57BL/6J mice (4–6 weeks old, 20 $\pm$ 2 g) were purchased from Beijing Vital River Laboratory Animal Technology Co., Ltd. (Beijing, China) and maintained on a 12 h light/12 h dark cycle at a constant temperature of 24 °C. The whole experiments were performed continually for 16 weeks. In the first 12 weeks, the mice were fed either on standard chow diet (SCD) ( $n=6$ ) or HFD (68.5% standard diet, 15% lard, 1% cholesterol, 0.5% bile and 15% dextrin) ( $n=18$ ) [36]. At week 13, the HFD fed mice were further divided into 3 groups randomly, including HFD group, HFD plus API (50 mg/kg) group and HFD plus ALL (5 mg/kg) group ( $n=6$ ). The drugs were administered by gavage every day. Mice were weighed weekly until sacrificed. Animal welfare and experimental procedures were followed in accordance with the ethical regulations of Nanjing Agricultural University (Permission Number: SYXK (Su) 2017–0007).

### 2.3. Hematoxylin–eosin (HE) and oil red O staining

In order to investigate histological change, liver tissue was embedded by paraffin and cut into 5  $\mu$ m serial sections, and then subjected to standard HE staining. For determination of hepatic fat accumulation, 8  $\mu$ m frozen liver sections were sequentially stained with Oil Red O and hematoxylin according to standard methods. For analysis of

intracellular lipid accumulation, cells in 6-well plates were washed with PBS and fixed with 10% neutral formalin, followed by staining with Oil Red O and hematoxylin.

### 2.4. Cell viability assay

Hepa1–6 cells ( $1\times 10^4$ ) were seeded in 96-well plates, then treated with various concentrations of API (0–512  $\mu$ M) for 24 h [29]. Adherent cells were analyzed by MTT assay and detected by Microplate reader (Biotek, Vermont, USA).

### 2.5. Cell culture and drug treatment

The murine hepatoma Hepa1–6 cell line was obtained from the Chinese Academy of Science. Cells were grown in DMEM (supplemented with 10% FBS, 1% penicillin/streptomycin and 1 mM Sodium Pyruvate Solution) at 37 °C, with 5% CO $_2$  atmosphere. In order to establish a cellular model of hepatic steatosis, cells were treated for 48 h with a mixture of free fatty acids (FFA) (oleate and palmitate in a final ratio of 2:1) at a final concentration of 0.5 mM. To evaluate the effects of API, during the treatment (at 24 h), these cells were exposed to different concentrations of API (16 and 32  $\mu$ M) or ALL (2  $\mu$ M).

### 2.6. Insulin tolerance tests (ITTs) and glucose tolerance test (GTTs)

For ITTs, mice were injected intraperitoneally with insulin solution (1 mU/g body weight) after a 6 h fast. For GTTs, mice were injected intraperitoneally with glucose solution (1 mg/g body weight) after a 16 h fast. Blood glucose levels were measured using a freestyle brand glucometer.

### 2.7. RNA isolation and real-time PCR

Total RNA was extracted as usual from liver tissues or cells and reverse transcribed to cDNA. A Light Cycler instrument (Roche, Mannheim, Germany) and an AceQ qPCR SYBR Green I kit (Vazyme, Nanjing, China) were used for real-time PCR analysis. The whole system of RT-PCR including the cDNA sample (1  $\mu$ L), PCR Mix (10  $\mu$ L), primers (2  $\mu$ L of each primer), and double-distilled H $_2$ O (7  $\mu$ L). The optimal PCR conditions were 35 cycles of 92 °C for 30 s, 58 °C for 60 s, and 72 °C for 30 s. Relative mRNA expression of target genes was obtained by normalizing to control group or SCD group and the level of  $\beta$ -actin, by using 2 $^{-\Delta\Delta Ct}$  method.

### 2.8. Western blot and immunohistochemistry

Total proteins were extracted from cells and liver tissues using RIPA buffer supplemented with protease and phosphatase inhibitors and separated by 10–12% SDS-PAGE, followed by transferring to 0.45- $\mu$ m polyvinylidene fluoride (PVDF) membranes (GE Healthcare, Marlborough, USA). Membranes were pre-blocked with 5% non-fat dry milk in TBST, followed by incubation overnight with the following primary antibodies: NLRP3, ASC, Pro-caspase-1, Caspase-1, and  $\beta$ -actin. The immunoglobulin G (IgG) anti-rabbit-HRP was applied. Amersham Imager 600 (GE Healthcare, Marlborough, USA) was used to visualize chemo-luminescence.

Immunohistochemistry was performed for macrophages and Kupffer cells recruitment studies. For details, liver tissue sections were dewaxed, dehydrated, rehydrated and antigen retrieval in citrate buffer. Then endogenous peroxidase activity was blocked for 10 min using 3.0% hydrogen peroxide. After blocked for 30 min using 10% goat plasma, the sections were separately incubated with primary antibodies against F4/80 at 4 °C overnight. The primary antibody was detected using biotinylated secondary antibodies (Servicebio, Wuhan, China). The staining of the sections was performed using streptavidin-HRP conjugates (Servicebio, Wuhan, China) for F4/80. Immunospecific reactivity was visualized by peroxidase oxidation of diaminobenzidine sub strate (DAB; Servicebio, Wuhan, China), counterstained with hematoxylin (Jiancheng, Nanjing, China), then dehydrated in alcohol and xylene and mounted onto glass slides [37]. F4/80-positive staining was used to identify activated macrophages and Kupffer cells surrounding steatotic hepatocytes. Sections were imaged at 400 $\times$  magnification (Olympus, Japan).

### 2.9. Immunofluorescence

Hepa1–6 cells were fixed in 40% paraformaldehyde for 30 min after incubated with 5% bovine serum albumin, specific primary antibodies were added. The cells were incubated overnight at 4 °C or 1 h at 37 °C in a humidified chamber. After being washed with PBS, the cells were then incubated in DAPI for 10 min at 37 °C. Cells were visualized under a confocal scanning microscope (Nikon, Kawasaki, Japan).

### 2.10. Statistical analysis

The data were expressed as the mean $\pm$ S.E.M. The statistical significance of the differences between treatment groups and the control group was determined using Student's *t*-test. A *P*-value of  $\leq 0.05$  was considered statistically significant.

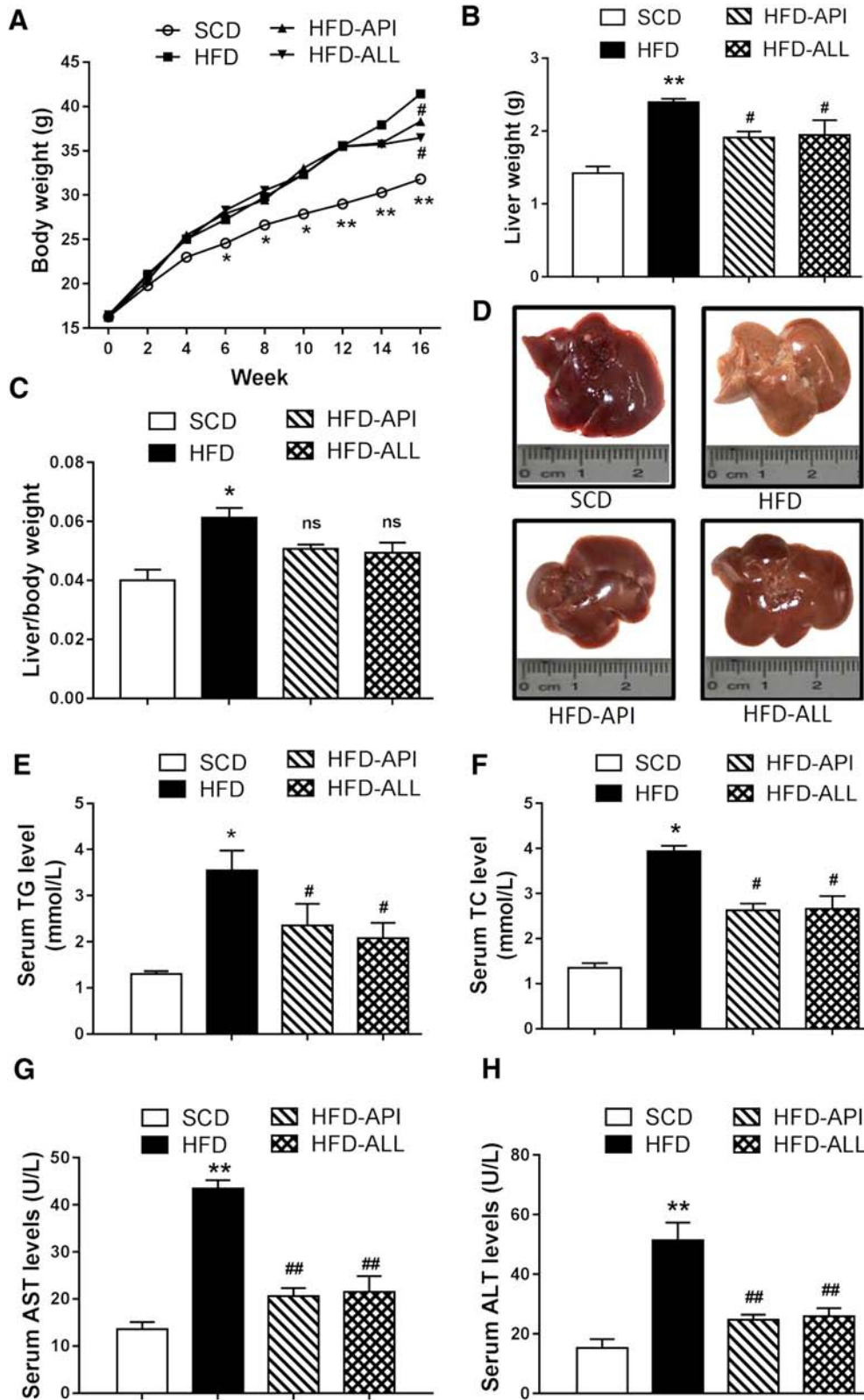


Fig. 1. API attenuates HFD-induced liver injury and obesity in HFD-fed mice. (A) Body weight of mice. (B) The effect of API on mice liver weight change. (C) The effect of API on mice liver/body weight. (D) Representative morphological images of liver tissue. (E-F) Serum levels of TG and TC. (G-H) Serum levels of AST and ALT. The results represent the mean  $\pm$  S.E.M. ( $n=6$ ). \* $P<.05$ , \*\* $P<.01$  vs. the SCD group; # $P<.05$ , ## $P<.01$  vs. the HFD group.

### 3. Results

#### 3.1. API decreases weight gain and liver injury in HFD-fed mice

As shown in Fig. 1, compared with the SCD group, HFD could increase body weight, and the weight of liver and ratio of liver weight/body weight were all increased for HFD fed mice. API treatment could recover the weight change (Fig. 1A–C). Furthermore, the liver color of the mice fed with HFD for 16 weeks became yellowish-brown compared with SCD group, which could also be reversed by API (Fig. 1D). In addition, TG, TC, AST and ALT levels were detected, which further demonstrated the protective effect of API on HFD-induced hepatic injury (Fig. 1E–H).

#### 3.2. API improves insulin sensitivity and glucose metabolism in HFD mice

Insulin tolerance tests (ITTs) and glucose tolerance tests (GTTs) *in vivo* were performed to characterize whether API could improve hepatic insulin resistance. As shown in Fig. 2A, mice fed with HFD significantly impaired glucose metabolism compared with SCD-fed mice, but API treatment improved glucose metabolism during the GTTs. The area under the curve of GTTs also revealed that glucose tolerance is improved in HFD-fed mice after API treatment (Fig. 2B). In line with GTTs, during the ITTs, mice fed with HFD significantly decreased insulin sensitivity, which could be improved by API (Fig. 2C–D).

#### 3.3. API ameliorates hepatic steatosis and regulates expression of lipid metabolism genes associated with NAFLD

As shown in Fig. 3A–B, hepatic steatosis and lipid accumulation induced by HFD could be significantly reduced by API. So does the liver steatosis score (Fig. 3C). Meanwhile, changes of intrahepatic TG and MDA further confirmed the effect of API on HFD-induced lipid

accumulation and lipid peroxidation (Fig. 3D–E). To investigate the mechanism that API exerts its protection against hepatic steatosis and lipid accumulation in HFD-fed mice, we examined the expression of several key regulators involved in lipid metabolism. Our results showed that, with the addition of API, the mRNA levels of lipogenic genes sterol regulatory element binding protein-1c (Srebf1), fatty acid synthase (Fasn), peroxisome proliferator-activated receptor gamma (PPAR- $\gamma$ ) (Fig. 3F), and lipid uptake related genes fatty acid binding protein-1 genes (Fabp-1) and lipoprotein lipase (Lpl) were downregulated (Fig. 3G). Additionally, fatty  $\beta$ -oxidation genes, such as peroxisome proliferator-activated receptor  $\alpha$  (PPAR- $\alpha$ ) and carnitine palmitoyltransferase-1  $\alpha$  (Cpt1- $\alpha$ ) were also decreased by API treatment compared with mice fed with HFD alone (Fig. 3H). In our study, antioxidant stress response-related genes NAD(P)H: quinone oxidoreductase 1 (NQO1), heme oxygenase-1 (HO-1) and glutathione S-transferase class Alpha2 (Gsta-1) (Gsta-1) were also detected, which indicated that API treatment could improve oxidative stress levels of HFD-fed mice (Fig. 3I). All these observations suggested that API could effectively inhibit fat accumulation and lipid peroxidation in HFD-induced mice.

In addition, we also established an *in vitro* model of NAFLD using FFA. The results showed that API under the dosages of 64  $\mu$ M had no toxicity on the viability of Hepa1–6 cells (Fig. 4A). The influence of API on intracellular fat accumulation in Hepa1–6 cells was confirmed by intracellular TG accumulation and Oil Red O staining. As shown in Fig. 4B and C, API treatment significantly attenuated FFA-stimulated intracellular lipid accumulation. In line with the results *in vivo*, API could partially (significantly) deregulate the lipid metabolism-related gene expression in Hepa1–6 cells (Fig. 4D–H). Collectively, these observations demonstrated that API could effectively inhibit lipid accumulation and regulate lipid metabolism both *in vivo* and *in vitro*.

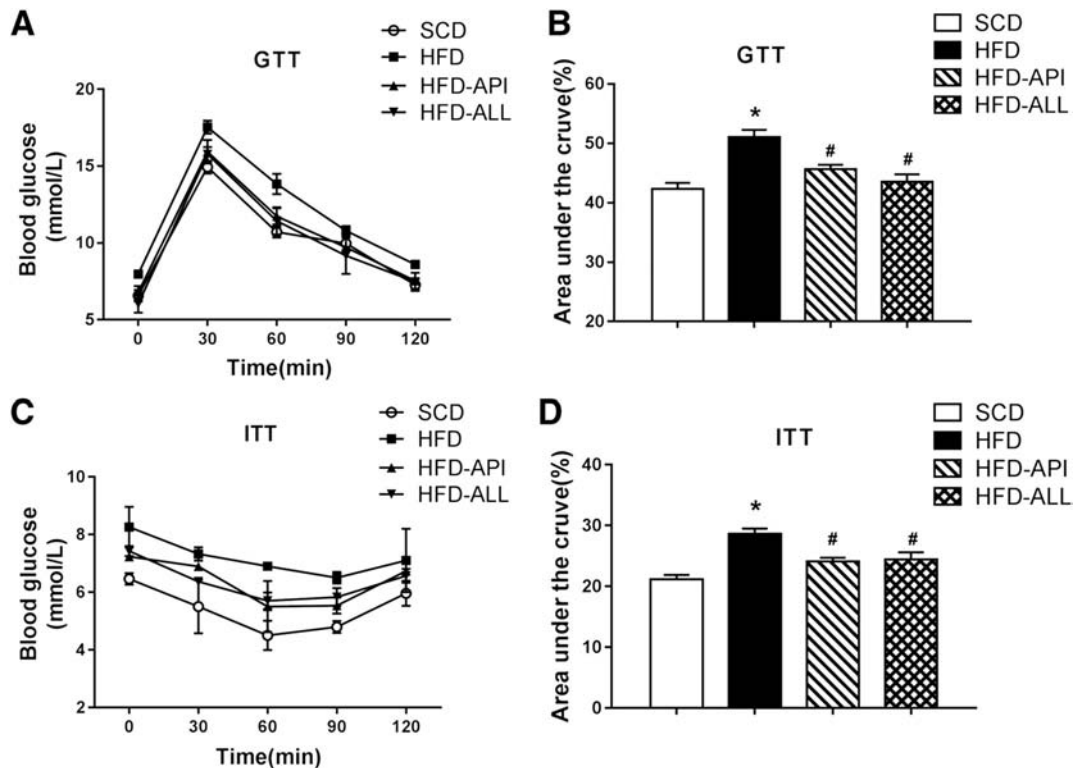


Fig. 2. API ameliorates insulin sensitivity and glucose tolerance in HFD-fed mice. (A) Glucose tolerance test (GTTs) for mice. (B) The area under the curve of GTT. (C) Insulin tolerance test (ITTs) for mice. (D) The area under the curve of ITT. The data are expressed as the mean  $\pm$  S.E.M. (n=3). \*P<.05, vs. SCD group; #P<.05, vs. the HFD group.

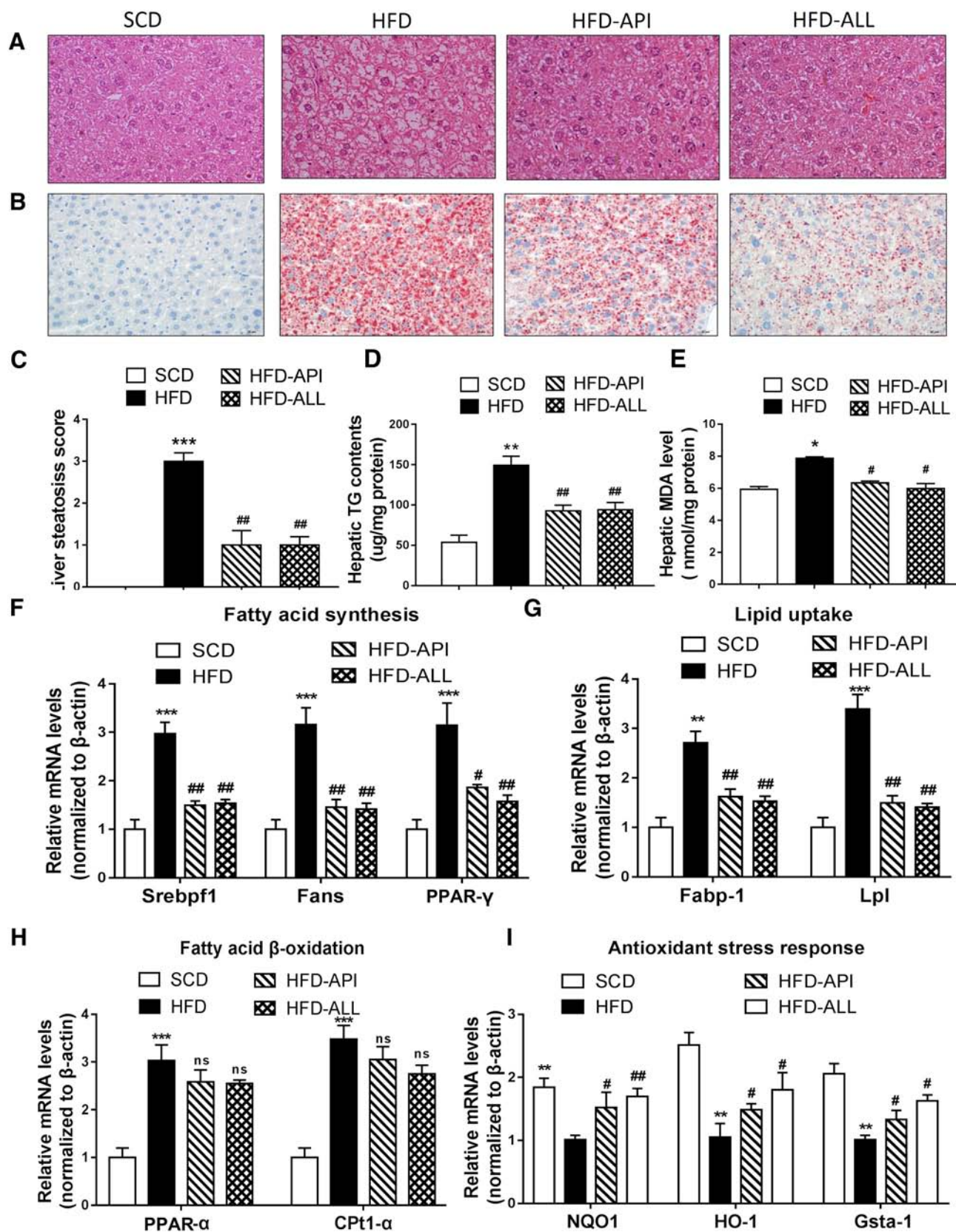


Fig. 3. API reduces intracellular lipid accumulation and expression of genes affecting lipid metabolism and oxidative stress associated with NAFLD in HFD-fed mice. (A-B) Liver histology as determined by H&E and Oil Red O staining. Original magnification  $\times 400$ . (C) Hepatic steatosis score. Score according to the grade of the lesion, slight (0.5), mild (1), moderate (2), severe (3), profound severe (4) and normal (0), ( $n=6$ ) (D) Hepatic TG content. (E) Hepatic levels of MDA. (F-I) Quantitative real-time PCR determination of hepatic mRNA expression of genes involved in the fatty acid synthesis, lipid uptake, fatty acid  $\beta$ -oxidation, and antioxidant stress response respectively. The data are expressed as the mean  $\pm$  S.E.M. ( $n=6$ ). \* $P<.05$ , \*\* $P<.01$ , \*\*\* $P<.001$  vs. the SCD group; # $P<.05$ , ## $P<.01$  vs. the HFD group.

### 3.4. API could inhibit HFD-induced macrophages recruitment and inflammation

HFD could increase the number of Kupffer cells [38], and proinflammatory mediators secreted by Kupffer cells played an important role in the initiation of NAFLD [39]. As shown in Fig. 5A–C, the mRNA levels of inflammatory cytokines Interleukin-6 (IL-6), chemokine (C-C motif) ligand 2 (Ccl2) and chemokine (C-C motif) receptor 2 (Ccr2) in the liver of HFD-fed mice were significantly improved and these parameters could be reduced by API. Likely, relevant mRNA of macrophage markers, including F4/80, Cd11b, and Cd68 were also re-balanced with API in HFD-fed mice liver (Fig. 5D–F). In the study, F4/80-positive staining was used to identify kupffer cells. As shown in Fig. 5G, crown-like structure (CLS) of kupffer cells was formed surrounding steatotic hepatocytes in the liver of HFD-fed mice (Fig. 5G). However, API could significantly correct the overexpression of these inflammatory markers and macrophages infiltration. Additionally, IL-1 $\beta$  and IL-18 mRNA expression and release were also detected in HFD-fed mice serum and liver in our study, which further verified the function of API (Fig. 5H–M). Taking together, our studies indicated that API could attenuate HFD-induced inflammation response.

### 3.5. API protection against NAFLD involves the activity of XO inhibition

It is reported that XO is a critical regulator of NAFLD and may serve as a novel therapeutic target for NAFLD [13]. Our results showed that, with the increasing of hepatic lipid accumulation and inflammation response, the XO activity was also significantly increased in HFD-induced mice, which could be remarkably inhibited by API or ALL (a clinically approved XO inhibitor, as a positive control drug in our study) (Fig. 6A). Meanwhile, inhibiting XO activity by API could dramatically attenuate serum, intrahepatic uric acid levels, and intrahepatic ROS level (Fig. 6B–D). Likely, the XO activity and ROS level in FFA-stimulated hepa1–6 cell were markedly decreased when treated with API (Fig. 6E). Meanwhile, the enhanced fluorescence intensity of DCF in FFA-stimulated Hepa1–6 cells was significantly reduced by API treatment (Fig. 6F–G), which suggested that API was a potent inhibitor of XO in models of NAFLD.

### 3.6. NLRP3 inflammasome-mediated protection of API against NAFLD

It has been reported that XO could regulate the activation of the NLRP3 inflammasome [25], which plays a crucial role in various metabolic diseases including NAFLD [27,40,41]. We, therefore, speculated that API might regulate NAFLD by inhibiting XO activity, which further inhibits NLRP3 inflammasome activation. In this research, API or ALL treatment could significantly down-regulate the mRNA and protein expression of NLRP3, ASC, Pro-caspase-1, caspase-1 in HFD-fed mice (Fig. 7A, C). The same results were obtained *in vitro* study (Fig. 7B, E). The western blot analyses *in vivo* and *in vitro* were further quantified by densitometry (Fig. 7D and Fig. 7F), respectively. In addition, the influence of API on NLRP3 inflammasome assembly on FFA-stimulated hepa1–6 cells was analyzed by immunofluorescence staining. As shown in Fig. 7G, confocal microscopic analysis showed the increased expression and co-localization of NLRP3, ASC, and Caspase-1 in FFA-stimulated Hepa1–6 cells. However, the assembly of NLRP3 inflammasomes was blocked by API. Our results showed that API could inhibit XO activity, and further modulated uric acid production to prevent NLRP3 inflammasome activation and ameliorates hepatic steatosis.

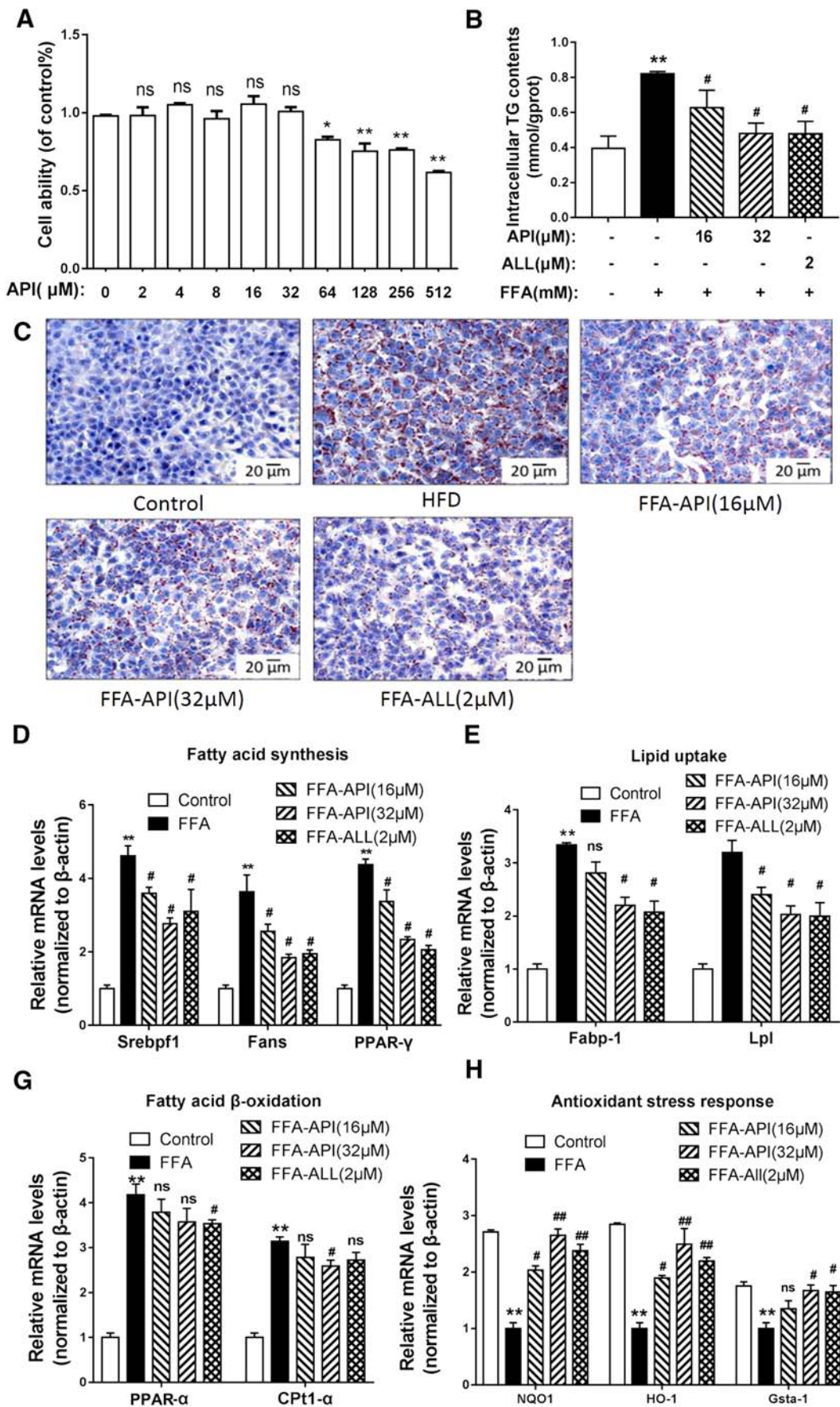
## 4. Discussion

XO, a rate-limiting enzyme predominantly expressed in liver, catalyzes the production of uric acid [12]. Recent studies have

demonstrated that XO is strongly associated with NAFLD-related disease, such as diabetes, atherosclerosis and so on [11,42]. Furthermore, XO activity is significantly elevated in NAFLD and obese patients [13,43]. Therefore, XO may play an important role in lipid peroxidation [44] and NAFLD [13]. The increase of the activity of XO will lead to the overproduction of ROS and uric acid, which may damage the liver due to oxidative stress and increased *de novo* lipogenesis in cultured cells [14,24]. In our study, the activity of XO was markedly increased in models of NAFLD. Similarly, ROS and uric acid levels in NAFLD models was higher than the normal group. We inhibited hepatic XO activity by ALL in HFD-fed mice and found that ALL significantly decreased uric acid and ROS levels in HFD-fed mice. A very relevant finding was that inhibiting XO activity could dramatically attenuate HFD-induced lipid accumulation and liver damage in mice. Thus, inhibiting XO activity in hepatocytes may be an effective method for treatment of fatty liver disease.

API (4, 5, 7-trihydroxyavone), is a kind of naturally occurring flavonoid [28], which has many pharmacological activities, such as antioxidant [29] and anti-cancer [31]. It is reported that API has the efficacy on inhibiting NAFLD progression by improving the oxidative stress and the lipid metabolism abnormality of liver [29] and API can attenuate obesity-related inflammation *via* regulation of macrophage polarization in mice [45]. However, the mechanism of API on NAFLD remains unclear. It has been reported that knocking down XO expression or inhibiting XO activity could attenuate hepatocyte fat accumulation in FFA-induced cells [13]. Additionally, the XO inhibitor, ALL, could meliorate hepatic steatosis through suppressing ROS formation in mice NAFLD model [40]. API was the most potent inhibitors of XO among tested flavonoids such as quercetin, myricetin and so on [46]. Molecular modeling revealed that hydroxyl moiety at C7 and C5 and the carbonyl group at C4 of API contribute favorable hydrogen bonds and electrostatic interactions between API and the active site of XO. Therefore, the relief of NAFLD by API may lie in its role on the regulation of the XO. Our results showed that the increase of XO activity induced by FFA/HFD *in vivo* and *in vitro* was significantly abolished by API treatment. Accordingly, intrahepatic and serum uric acid and ROS levels in mice models of NAFLD were reduced with API treatment. Uric acid and ROS, are two catalytic product of XO. Some studies have proven that uric acid can modulate lipid homeostasis in fatty liver by regulating mitochondrial function [14], while XO-derived mitochondrial ROS is the trigger for IL-1 $\beta$  release [25]. As we know, IL-1 $\beta$  increases the lipid accumulation in hepatocytes, induces hepatic insulin resistance and results in NAFLD [47]. In the present study, we found that API or ALL treatment could not only inhibit the activity of XO and reduced uric acid and ROS, but also ameliorated lipid accumulation of liver in HFD-fed mice and FFA-induced cells. Therefore hepatic lipid accumulation reduced by API may be due to the modulation of XO. It has been proven that many flavonoids could competitively inhibit the XO, such as API, quercetin, luteolin, myricetin, isovitexin and so on [46,48]. Among these compounds, API can be absorbed more efficiently in intestinal mucosa and eliminated slower in serum in spite of its possibly week XO inhibitory capacity [48–50]. Furthermore, API is relatively nontoxic and nonmutagenic, and it has gained importance as a beneficial and health promoting agent [51,52]. Additionally, no adverse metabolic reactions can be observed when consumed API as part of a normal diet [52]. Therefore, API is more suitable for clinical application than other flavonoids.

Inflammasomes are multiprotein complexes that trigger pro-inflammatory cytokines maturation, such as IL-1 $\beta$ , to engage innate immune defenses in response to cell infection and stress [22,53]. Among these inflammasome family, NLRP3 inflammasome is the most extensively studied and well-characterized member [27]. As reported, NLRP3 inflammasome activation results in a wide range of immune responses including production of pro-inflammatory cytokines [54,55], which subsequently accelerates the development of obesity [56], and obesity-related disease such as cardiovascular complications [57], type 2 diabetes [58], and NAFLD [17,59]. As the final product of hypoxanthine



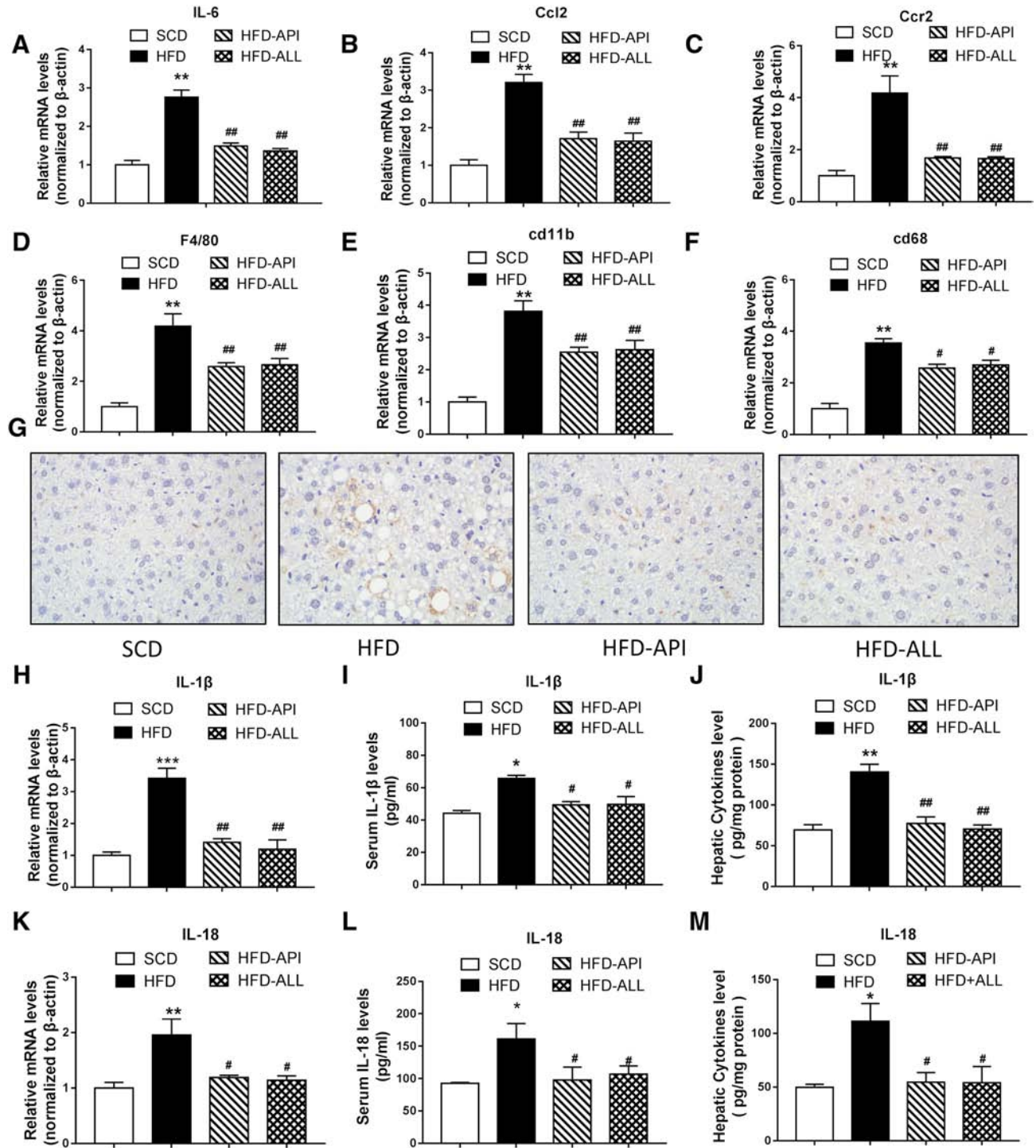


Fig. 5. HFD provokes IL-1 $\beta$  release and macrophages recruitment, which is inhibited by API. (A–C) Relative mRNA expression of IL-6, Ccl2, and Ccr2 in the liver of mice was detected by Quantitative real-time PCR. (D–F) Relative mRNA expression of macrophage markers such as F4/80, cd11b, and cd68 was detected by Quantitative real-time PCR. (G) F4/80 positive Kupffer cells measured by immunohistochemistry. Original magnification  $\times 400$ . (H) IL-1 $\beta$  mRNA level in mice liver. (I) Serum IL-1 $\beta$  level. (J) Hepatic IL-1 $\beta$  level. (K) IL-18 mRNA level in mice liver. (L) Serum IL-18 level. (M) Hepatic IL-18 level. IL-1 $\beta$  and IL-18 levels in serum or liver were used to determine with an ELISA. The data are expressed as the mean  $\pm$  S.E.M. ( $n = 6$ ). \* $P < .05$ , \*\* $P < .01$  vs. the SCD group; # $P < .05$ , ## $P < .01$  vs. the HFD group.

catalyzed by XO, uric acid and ROS participate in NLRP3 inflammasome activation and play an important role in the development of NAFLD and insulin resistance [27], which prompted us to investigate whether the

inhibition of XO by API could regulate NLRP3 inflammasome activation. In this study, we found that induction NAFLD in mice caused obvious NLRP3 expression and caspase-1 activation, together with the elevated

Fig. 4. API reduces intracellular lipid accumulation and expression of genes affecting lipid metabolism and oxidative stress associated with NAFLD in FFA-induced Hepa1–6 cells. (A) The effects of API on the viability of Hepa1–6 cells analyzed with MTT method. (B) Intracellular TG content. (C) Oil Red O staining of Hepa1–6 cells. Original magnification  $\times 200$ . (D–H) Quantitative real-time PCR determination of Hepa1–6 cells mRNA expression of genes involved in the fatty acid synthesis, lipid uptake, fatty acid  $\beta$ -oxidation, and antioxidant stress response respectively. Results are mean  $\pm$  S.E.M. of three independent experiments. \* $P < .05$ , \*\* $P < .01$  vs. the control group; # $P < .05$ , ## $P < .01$  vs. the FFA group.

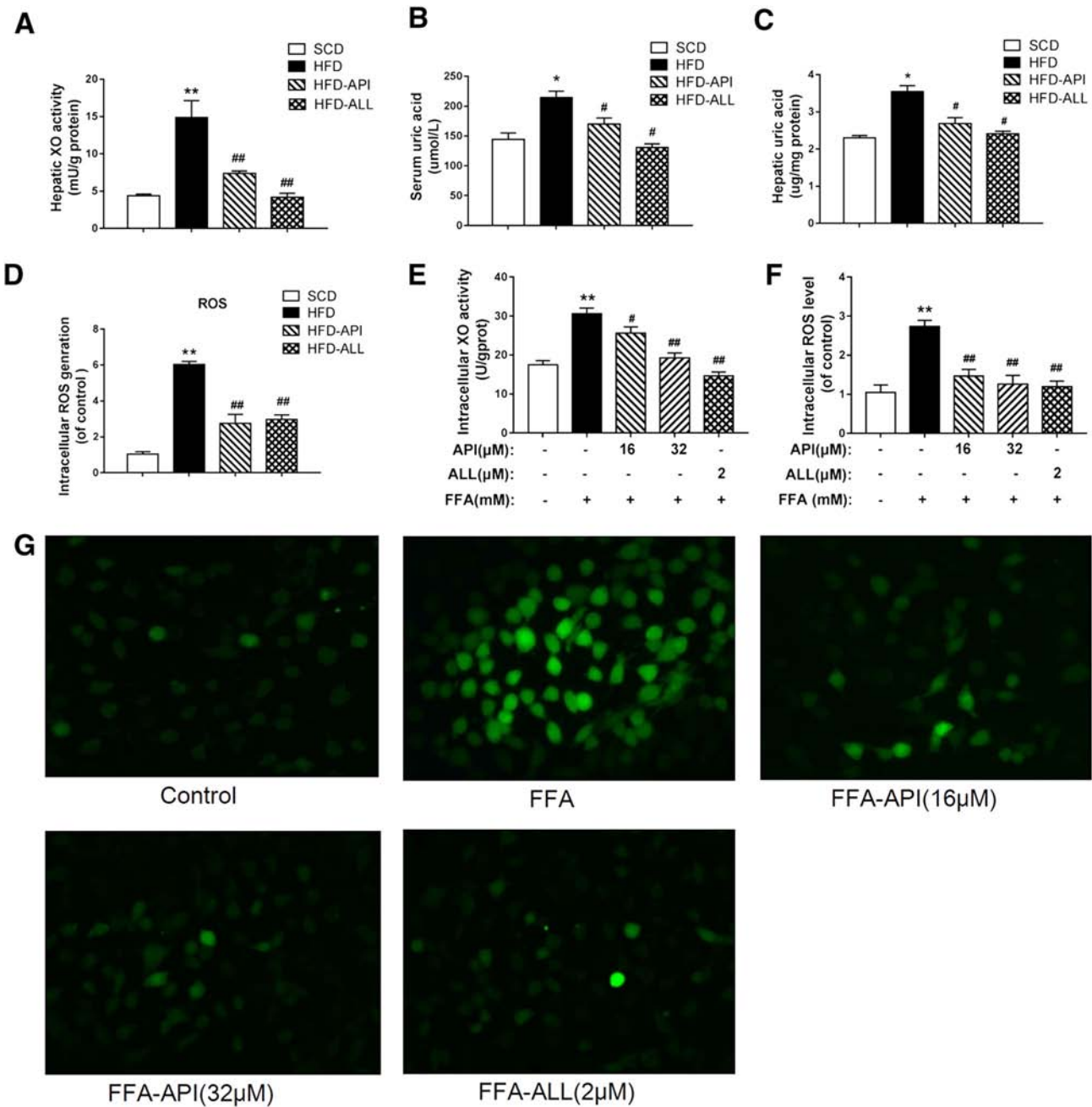


Fig. 6. API-mediated protection against NAFLD involves the activity of XO inhibition. (A) XO activity of liver tissue. (B–C) Serum and hepatic levels of uric acid. (D) Hepatic ROS level measured by fluorescent microplate. The data are expressed as the mean ± S.E.M. (n = 6). \*P < .05, \*\*P < .01 vs. the SCD group; #P < .05, ##P < .01 vs. the HFD group. (E) The activity of XO in Hepa1–6 cells. (F–G) Intracellular ROS level in Hepa1–6 cells in different groups measured under fluorescent microplate reader and fluorescence microscope. 200 × Original magnification. Results are mean ± S.E.M. of three independent experiments. \*P < .05, \*\*P < .01 vs. the control group; #P < .05, ##P < .01 vs. the FFA group.

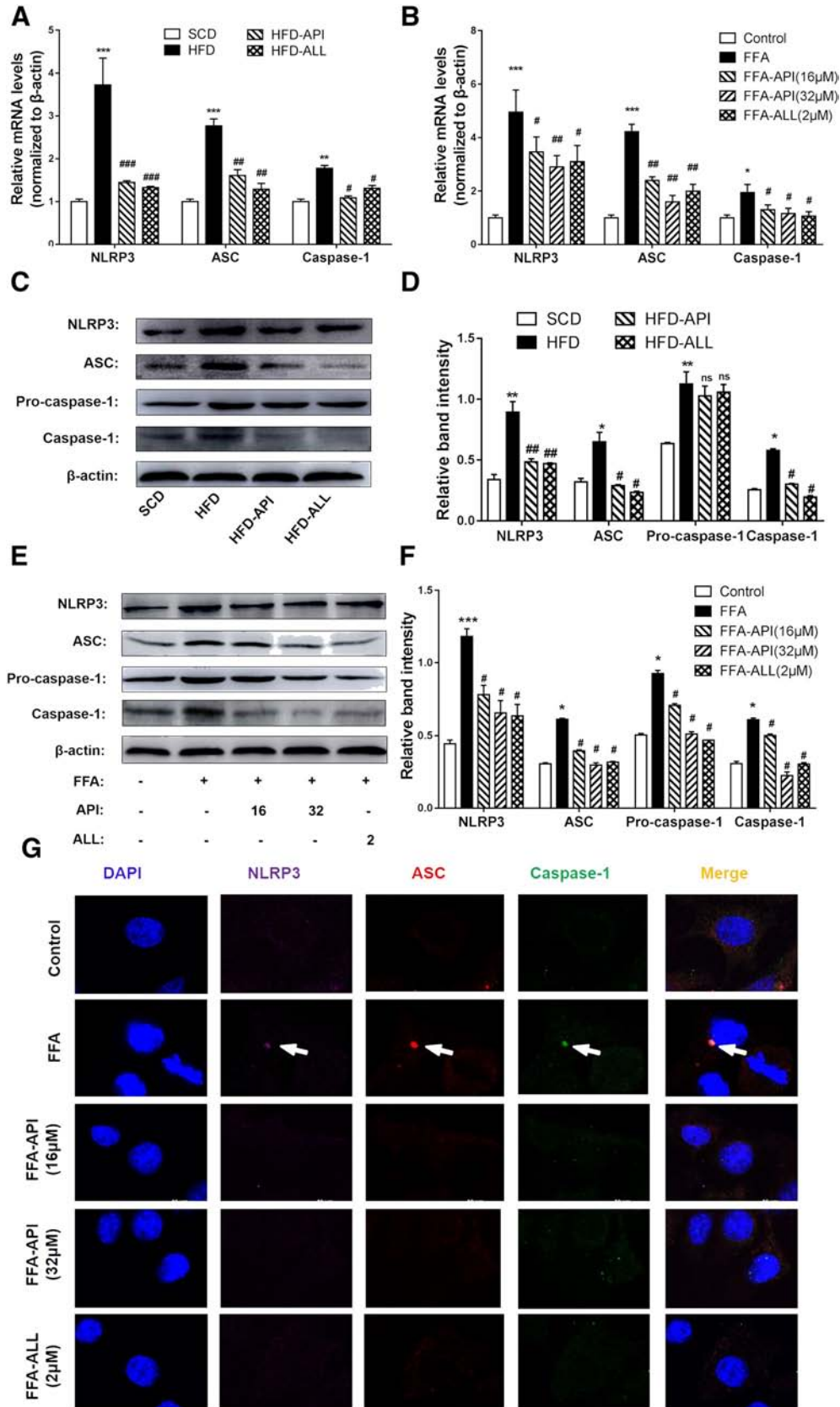
levels of IL-1β and IL-18 in the liver of HFD-fed mice model. While API treatment effectively suppressed the overexpression of NLRP3 and inhibited the activation of the NLRP3 inflammasome. The *in vitro* study further confirmed that API could be an NLRP3 inflammasome

modulator. These results suggested that the inhibitory effects of API on lipid accumulation and NLRP3 activation are partially mediated by XO. In addition, other mechanisms of API against NAFLD have been reported. For example, API can act as a modulator of PPARγ to attenuate

Fig. 7. API inhibits NLRP3 inflammasome activation to prevent the release of pro-inflammatory cytokines via XO activity regulation *in vivo* and *in vitro*. (A) NLRP3, ASC caspase-1 mRNA levels were determined by Quantitative real-time PCR in mice. (B) NLRP3, ASC caspase-1 mRNA levels were determined by Quantitative real-time PCR in Hepa1–6 cells. (C–D) NLRP3, ASC, pro-caspase-1, caspase-1 protein levels were detected by Western blots and quantified by using ImageJ software in mice. The data are expressed as the mean ± S.E.M. (n = 6). \*P < .05, \*\*P < .01, \*\*\*P < .001 vs. The SCD group; #P < .05, ##P < .01 vs. the HFD group. (E–F) NLRP3, ASC, Pro-caspase-1, caspase-1 protein levels were detected by Western blots and quantified by using ImageJ software in Hepa1–6 cells. (G) Immunocytochemistry of the subcellular localization of NLRP3 (purple), ASC (red) and caspase-1 (green) in Hepa1–6 cells. Blue, nuclei. Original magnification ×600. Results are mean ± S.E.M. of three independent experiments. \*P < .05, \*\*P < .01, \*\*\*P < .001 vs. the control group; #P < .05, ##P < .01, ###P < .001 vs. the FFA group.

HFD-induced NAFLD by regulating hepatocyte lipid metabolism and oxidative stress *via* Nrf2 activation [29]. Therefore, because of the complex pathogenesis of NAFLD, the relationship between API and NAFLD remains to be further explored.

In conclusion, API had the efficacy on suppressing hepatic steatosis, inhibiting inflammation and modulating the lipid metabolism in the liver, therefore preventing the NAFLD. The beneficial effects of API on NAFLD might be partly due to the fact that API could inhibit NLRP3



inflammasome assembly and activation by downregulating XO activity, inhibiting uric acid and ROS production. This effect further reduced the overproduction of pro-inflammatory cytokines IL-1 $\beta$  and IL-18, which stop the development of NAFLD. These observations proved that XO was a potential therapeutic target in the treatment of NAFLD and API was a beneficial and health-promoting agent on fatty liver disease.

## Acknowledgments

This work was supported by the National Key R&D Program (2016YFD0501009 and 2016YFD0501200), the Natural Science Foundation of Jiangsu Province (BK20161452), the Fundamental Research Funds for the Central Universities (KYZ201848), the Priority Academic Program Development of Jiangsu Higher Education Institutions, the NAU International Cooperation and Cultivation Project (2018-AF-20) and the Key Program of Science and Technology Planning of Guangdong Province (2017B020202010).

## Declaration of Competing Interest

The authors declare no conflicts of interest.

## References

- Ahmed MH. Non-alcoholic fatty liver disease (NAFLD): new challenge for general practitioners and important burden for health authorities? *Prim Care Diabetes* 2010;4:129–37.
- Loomba R, Sanyal AJ. The global NAFLD epidemic. *Nat Rev Gastroenterol Hepatol* 2013;9:686–90.
- Karlas T, Wiegand J, Berg T. Gastrointestinal complications of obesity: non-alcoholic fatty liver disease (NAFLD) and its sequelae. *Best Pract Res Clin Endocrinol Metab* 2013;27:195–208.
- Byrne CD, Targher G. NAFLD: a multisystem disease. *J Hepatol* 2015;62:S47–64.
- Birkenfeld AL, Shulman GI. Non alcoholic fatty liver disease, hepatic insulin resistance and type 2 diabetes. *Hepatology* 2014;59:713–23.
- Targher G, Byrne CD, Lonardo A, Zoppini G, Barbui C. Non-alcoholic fatty liver disease and risk of incident cardiovascular disease: a meta-analysis. *J Hepatol* 2016;65:589–600.
- Mantovani A, Zaza G, Byrne CD, Lonardo A, Zoppini G, Bonora E, et al. Nonalcoholic fatty liver disease increases risk of incident chronic kidney disease: a systematic review and meta-analysis. *Metabolism Clinical & Experimental* 2017;79:64–76.
- Dietrich MO, Horvath TL. Limitations in anti-obesity drug development: the critical role of hunger-promoting neurons. *Nat Rev Drug Discov* 2012;11:675–91.
- Harris CM, Massey V. The oxidative half-reaction of xanthine dehydrogenase with NAD: reaction kinetics and steady-state mechanism. *J Biol Chem* 1997;272:28335–41.
- Cheung KJ, Iphigenia T, Pavlos P, Ilsa R, Oksana G, Toshio O, et al. Xanthine oxidoreductase is a regulator of adipogenesis and PPAR $\gamma$  activity. *Cell Metab* 2007;5:115–28.
- Kushiya MA, Okubo H, Sakoda H, Kikuchi T, Fujishiro M, Sato H, et al. Xanthine oxidoreductase is involved in macrophage foam cell formation and atherosclerosis development. *Arterioscler Thromb Vasc Biol* 2012;32:291–8.
- Kurosaki M, Calzi ML, Scanziani E, Garattini E, Terao M. Tissue- and cell-specific expression of mouse xanthine oxidoreductase gene in vivo: regulation by bacterial lipopolysaccharide. *Biochem J* 1995;306:225–34.
- Xu C, Wan X, Xu L, Weng H, Yan M, Miao M, et al. Xanthine oxidase in non-alcoholic fatty liver disease and hyperuricemia: one stone hits two birds. *J Hepatol* 2015;62:1412–9.
- Lanaspa MA, Sanchez-Lozada LG, Yea-Jin C, Christina C, Mehmet K, Roncal-Jimenez CA, et al. Uric acid induces hepatic steatosis by generation of mitochondrial oxidative stress: potential role in fructose-dependent and -independent fatty liver. *J Biol Chem* 2012;287:40732–44.
- Li Y, Xu C, Yu C, Xu L, Miao M. Association of serum uric acid level with non-alcoholic fatty liver disease: a cross-sectional study. *J Hepatol* 2009;50:1029–34.
- Wang B, Yang RN, Zhu YR, Xing JC, Lou XW, He YJ, et al. Involvement of xanthine oxidase and paraoxonase 1 in the process of oxidative stress in nonalcoholic fatty liver disease. *Mol Med Rep* 2016;15:387–95.
- Wree A, McGeough MD, Peña CA, Schlattjan M, Li H, Inzaugarat ME, et al. NLRP3 inflammasome activation is required for fibrosis development in NAFLD. *J Mol Med* 2014;92:1069–82.
- Dixon LJ, Flask CA, Papouchado BG, Feldstein AE, Nagy LE. Caspase-1 as a central regulator of high fat diet-induced non-alcoholic steatohepatitis. *PLoS One* 2013;8:e56100.
- Szabo G, Csak T. Inflammasomes in liver diseases. *J Hepatol* 2012;57:642–54.
- Jan P, Shashi B, Timea C, Dora L, Karen K, Victoria M, et al. IL-1 receptor antagonist ameliorates inflammasome-dependent alcoholic steatohepatitis in mice. *J Clin Invest* 2012;122:3476–89.
- Dixon LJ, Michael B, Samjhana T, Papouchado BG, Feldstein AE. Caspase-1-mediated regulation of fibrogenesis in diet-induced steatohepatitis. *Lab Invest* 2012;92:713–23.
- Schroder K, Tschopp J. The Inflammasomes. *Cell* 2010;140:821–32.
- Gyongyi S, Jan P. Inflammasome activation and function in liver disease. *Nat Rev Gastroenterol Hepatol* 2015;12:387–400.
- Lozovoy MA, Simão AN, Panis C, Rotter MA, Reiche EM, Morimoto HK, et al. Oxidative stress is associated with liver damage, inflammatory status, and corticosteroid therapy in patients with systemic lupus erythematosus. *Lupus* 2011;20:1250–9.
- Annette I, Johji N, Fabio M, Thierry R, Didier LR, Miner JN, et al. Xanthine oxidoreductase regulates macrophage IL1 $\beta$  secretion upon NLRP3 inflammasome activation. *Nat Commun* 2015;6:6555.
- Mohamed L. Emerging inflammasome effector mechanisms. *Nat Rev Immunol* 2011;11:213–20.
- Wan X, Xu C, Lin Y, Lu C, Li D, Sang J, et al. Uric acid regulates hepatic steatosis and insulin resistance through the NLRP3 inflammasome-dependent mechanism. *J Hepatol* 2016;64:925–32.
- And KHM, Mohamed S. Flavonoid (myricetin, quercetin, kaempferol, luteolin, and apigenin) content of edible tropical plants. *Journal of Agricultural & Food Chemistry* 2001;49:3106–12.
- Feng X, Wen Y, Li X, Zhou F, Zhang W, Qi S, et al. Apigenin, a modulator of PPAR $\gamma$ , attenuates HFD-induced NAFLD by regulating hepatocyte lipid metabolism and oxidative stress via Nrf2 activation. *Biochem Pharmacol* 2017;136:49.
- Je-Hyuk L, Yu ZH, So Yean C, Yeong Shik K, Soo LY, Choon Sik J. Anti-inflammatory mechanisms of apigenin: inhibition of cyclooxygenase-2 expression, adhesion of monocytes to human umbilical vein endothelial cells, and expression of cellular adhesion molecules. *Arch Pharm Res* 2007;30:1318–27.
- Shao H, Jing K, Mahmoud E, Huang H, Fang X, Yu C. Apigenin sensitizes colon cancer cells to antitumor activity of ABT-263. *Mol Cancer Ther* 2013;12:2640–50.
- Li R, Wang X, Qin T, Qu R, Ma S. Apigenin ameliorates chronic mild stress-induced depressive behavior by inhibiting interleukin-1 $\beta$  production and NLRP3 inflammasome activation in the rat brain. *Behav Brain Res* 2016;296:318–25.
- Mafuyu O, Ko F. Antiadipogenic effect of dietary apigenin through activation of AMPK in 3T3-L1 cells. *J Agric Food Chem* 2011;59:13346–52.
- Kim MA, Kang K, et al. Apigenin isolated from *Daphne genkwa* Siebold et Zucc. Inhibits 3T3-L1 preadipocyte differentiation through a modulation of mitotic clonal expansion. *Life Sci* 2014;101:64–72.
- Carlos E, Veronica N, Nathan LP, Verena C, Ana PG, Maria Thereza B, et al. Flavonoid apigenin is an inhibitor of the NAD $^{+}$  ase CD38: implications for cellular NAD $^{+}$  metabolism, protein acetylation, and treatment of metabolic syndrome. *Diabetes* 2013;62:1084–93.
- Cui Y, Wang Q, Li X, Zhang X. Experimental nonalcoholic fatty liver disease in mice leads to cytochrome p450 2a5 upregulation through nuclear factor erythroid 2-like 2 translocation. *Redox Biol* 2013;1:433–40.
- Tu K, Zheng X, Yin G, Zan X, Yao Y, Liu Q. Evaluation of Fbxw7 expression and its correlation with expression of SREBP-1 in a mouse model of NAFLD. *Mol Med Rep* 2012;6:525–30.
- Tongfang T, Yongheng S, Min L, Zhiping L, Jing H. Pro-inflammatory activated Kupffer cells by lipids induce hepatic NKT cells deficiency through activation-induced cell death. *PLoS One* 2013;8:e81949.
- disease Katherine S Liver. Kupffer cells regulate the progression of ALD and NAFLD. *Nat Rev Gastroenterol Hepatol* 2013;10:503.
- Zhang X, Zhang JH, Chen XY, Hu QH, Wang MX, Jin R, et al. ROS-induced TXNIP drives fructose-mediated hepatic inflammation and lipid accumulation through NLRP3 inflammasome activation. *Antioxid Redox Signal* 2015;22:848–70.
- Mridha AR, Wree A, Robertson AAB, Yeh MM, Johnson CD, Rooyen DMV, et al. NLRP3 inflammasome blockade reduces liver inflammation and fibrosis in experimental NASH in mice. *J Hepatol* 2017;66:1037–46.
- Marí-Carmen D, Miguel A, Rafael M, José MV, Máximo V, Pallardó FV, et al. Xanthine oxidase is involved in free radical production in type 1 diabetes: protection by allopurinol. *Diabetes* 2002;51:1118–24.
- Juanwen Z, Chengfu X, Ying Z, Yu C. The significance of serum xanthine oxidoreductase in patients with nonalcoholic fatty liver disease. *Clin Lab* 2014;60:1301–17.
- Kato S, Kawase T, Alderman J, Inatomi N, Lieber CS. Role of xanthine oxidase in ethanol-induced lipid peroxidation in rats. *Gastroenterology* 1990;98:203–10.
- Feng X, Weng D, Zhou F, Owen YD, Qin H, Zhao J, et al. Activation of PPAR $\gamma$  by a natural flavonoid modulator, Apigenin ameliorates obesity-related inflammation via regulation of macrophage polarization. *EBioMedicine* 2016;9:61–76.
- Lin CM, Chen CS, Chen CT, Liang YC, Lin JK. Molecular modeling of flavonoids that inhibits xanthine oxidase. *Biochem Biophys Res Commun* 2002;294:167–72.
- Tilg H, Moschen AR. IL-1 cytokine family members and NAFLD: neglected in metabolic liver inflammation. *J Hepatol* 2011;55:960–2.
- Qi J, Sun LQ, Qian SY, Yu BY. A novel multi-hyphenated analytical method to simultaneously determine xanthine oxidase inhibitors and superoxide anion scavengers in natural products. *Anal Chim Acta* 2017;984:124–33.
- Chen T, Li L, Lu X, Jiang H, Su Z. Absorption and excretion of luteolin and apigenin in rats after oral administration of *Chrysanthemum morifolium* extract. *Journal of Agricultural & Food Chemistry* 2009;55:273–7.

- [50] Mo S, Zhou F, Lv Y, Hu Q, Kong L. Hypouricemic action of selected flavonoids in mice: structure-activity relationships. *Biol Pharm Bull* 2007;30:1551–6.
- [51] Lepley DM, Li B, Birt DF, Pelling JC. The chemopreventive flavonoid apigenin induces G2/M arrest in keratinocytes. *Carcinogenesis* 1996;17:2367–75.
- [52] Ali F, Rahul Naz F, Jyoti S, Siddique YH. Health functionality of apigenin: a review. *International Journal of Food Properties* 2017;20:1197–238.
- [53] Leemans JC, Cassel SL, Sutterwala FS. Sensing damage by the NLRP3 inflammasome. *Immunol Rev* 2011;243:152–62.
- [54] Broderick L, De ND, Franklin BS, Hoffman HM, Latz E. The Inflammasome and autoinflammatory syndromes. *Annu Rev Pathol* 2014;10:395–424.
- [55] Wree A, Broderick L, Canbay A, Hoffman HM, Feldstein AE. From NAFLD to NASH to cirrhosis-new insights into disease mechanisms. *Nat Rev Gastroenterol Hepatol* 2013;10:627–36.
- [56] Vandanmagsar B, Youm YH, Ravussin A, Galgani JE, Stadler K, Mynatt RL, et al. The NLRP3 inflammasome instigates obesity-induced inflammation and insulin resistance. *Nat Med* 2011;17:179–88.
- [57] Duewell P, Kono H, Rayner KJ, Sirois CM, Vladimer G, Bauernfeind FG, et al. NLRP3 inflammasomes are required for atherogenesis and activated by cholesterol crystals. *Nature* 2010;464:1357–61.
- [58] Masters SL, Dunne A, Subramanian SL, Hull RL, Tannahill GM, Sharp FA, et al. Activation of the NLRP3 inflammasome by islet amyloid polypeptide provides a mechanism for enhanced IL-1 $\beta$  in type 2 diabetes. *Nat Immunol* 2010;11:897–904.
- [59] Henaomejia J, Elinav E, Jin C, Hao L, Mehal WZ, Strowig T, et al. Inflammasome-mediated dysbiosis regulates progression of NAFLD and obesity. *Nature* 2012;482:179–85.